Formation of Ruthenium(II) Complexes with Unsymmetrical Terdentate Ligands

Yurngdong Jahng,[1a,b] Randolph P. Thummel,*[,1a] and Simon G. Bott[1c]

Departments of Chemistry, University of Houston, Houston, Texas 77204-5641, and University of North Texas, Denton, Texas 76203-0068

Received August 29, 1996[⊗]

Three unsymmetrical terdentate ligands, 2-(2′-quinolyl)-1,10-phenanthroline (**4**), 2-(1′-isoquinolyl)-1,10-phenanthroline (**5**), and 3,3′-dimethylene-2-(2′-quinolyl)-1,10-phenanthroline (**6**), have been prepared by application of the Friedländer condensation. Ligand **4** forms predominantly a pentaaza-coordinated (N5) complex with Ru(II), [Ru(**4**-*N*,*N*′,*N*′′)(**4**-*N*,*N*′)Cl](PF$_6$), whose structure was determined by X-ray analysis ($C_{42}H_{26}ClF_6N_6PRu$: monoclinic, *C*2/*c*, $a = 29.308(3)$ Å, $b = 15.205(2)$ Å, $c = 19.505(2)$ Å, $\beta = 107.312(8)°$, $V = 8298(1)$ Å^3, $Z = 8$). Ligand **5** forms predominantly a hexaaza-coordinated (N6) complex, [Ru(**5**-*N*,*N*′,*N*′′)$_2$](PF$_6$)$_2$. The bridged species **6** shows intermediate behavior, and the rate for interconversion of the N5 to N6 complex has been measured. The stereochemical features of these two binding modes are examined, and both π-stacking and steric effects are invoked to explain the observed behavior, leading to the proposal of a backside displacement mechanism for their interconversion.

Introduction

The use of 2,2′-bipyridine (bpy) and 2,2′:6,2′′-terpyridine (tpy) in the formation of octahedral complexes of d_6 metals such as ruthenium(II) has been widely exploited in recent years.[2] Although the formation of [Ru(tpy)$_2$]$^{2+}$ is generally thought to involve the stepwise reaction of tpy with RuCl$_3$·3H$_2$O, the actual coordination process has not been carefully examined. We were surprised to discover that this process is somewhat more complicated than it may appear, and this report discusses our findings.

Several examples of coordination with Ru(II) are known in which tpy does not utilize its maximum denticity. Two of these complexes are of the type [Ru(CO)$_2$(LL)(tpy-*N*,*N*)]$^{2+}$, where LL = Br, Br[3] or LL = 1,10-phenanthroline.[4] Group VI metals are also known to from bidentate tpy complexes of the type [M(CO)$_4$(tpy-*N*,*N*)].[5] A fluxional system has been discussed in which the metal moves from one bidentate tpy site to the other.[6] When insufficient sites are available on Ru(II), as in the reaction of of tpy with [Ru(bpy)$_2$Cl$_2$], the expected complex [Ru(bpy)$_2$(tpy-*N*,*N*′)]$^{2+}$ is formed.[7] The two available modes of coordination with [Ru(tpy)Cl$_3$] have been demonstrated by the reaction with 6-phenyl-2,2′-bipyridine which binds either terdentate *via* cyclometalation or bidentate to provide [Ru(tpy)(LL)Cl]$^+$.[8]

In the formation of [Ru(tpy)$_2$]$^{2+}$ from the reaction of tpy with [RuCl$_3$(H$_2$O)$_3$] in ethanol, the first tpy coordinates faster than the second as is demonstrated by the formation of [Ru(tpy)Cl$_3$] as the major product from a 1:1 reaction.[9] The tpy coordinates in a meridianal fashion (see Scheme 1), and thus, there is no stereochemistry associated with the 1:1 adduct. This intermediate species **1** has one equatorial and two axial leaving groups, and the second attacking tpy has two different nucleophilic sites, the central and the two distal pyridine rings. On steric, electronic, and statistical grounds, the distal pyridines should be more nucleophilic. Therefore the structure of the final product (**2** or **3**) will depend upon whether attack by a distal pyridine of tpy is favored at an axial or equatorial site on intermediate **1**.

Scheme 1

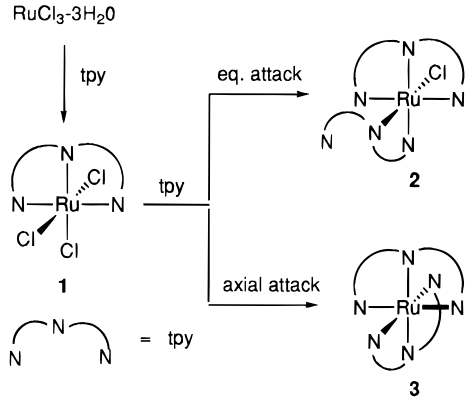

When the reaction illustrated in Scheme 1 is run under mild conditions in the absence of light, TLC analysis (Al$_2$O$_3$, CH$_3$CN/EtOH (19:1)) of the reaction mixture indicates the presence of the expected red bis-complex **3** with an $R_f = 0.3$ as well as a pink material with an $R_f = 0.4$. If the crude product mixture is analyzed by NMR, the presence of a small peak at δ 10.5 (CD$_3$CN) is observed. This peak is diagnostic of a tpy H$_6$ proton which is held in the deshielding region of the adjacent chlorine (Figure 1). If this signal is counted as one proton, it can be estimated that **2** and **3** are present in a ratio of about 1:20. Attempts to isolate **2** result in its isomerization to **3**. An earlier report of this same reaction in glacial acetic acid does not

⊗ Abstract published in *Advance ACS Abstracts,* June 15, 1997.

(1) (a) University of Houston. (b) On leave from Yeungnam University, Kyungsan, Korea. (c) University of North Texas.
(2) (a) Kalyanasundaram, K. *Photochemistry of Polypyridine and Porphyrin Complexes*; Academic Press: San Diego, CA, 1992. (b) Juris, A.; Balzani, V.; Barigelletti, F.; Campagna, S.; Belser, P.; von Zelewsky, A. *Coord. Chem. Rev.* **1988**, *84*, 85.
(3) Deacon, G. B.; Patrick, J. M.; Skelton, B. W.; Thomas, N. C.; White, A. H. *Aust. J. Chem.* **1984**, *37*, 929.
(4) Thomas, N. C.; Fischer, J. *J. Coord. Chem.* **1990**, *21*, 119.
(5) Ganorkar, M. C.; Stiddard, M. H. B. *J. Chem. Soc.* **1965**, 5346.
(6) Abel, E. W.; Long, N. J.; Orrell, K. G.; Osborne, A. G.; Pain, H. M.; Sik, V. *J. Chem. Soc., Chem Commun.* **1992**, 303.
(7) Constable, E. C.; Hannon, M. J.; Cargill Thompson, A. M. W.; Tocher, D. A.; Walker, J. V. *Supramolecular Chem.* **1993**, *2*, 243.
(8) Constable, E. C.; Hannon, M. J. *Inorg. Chim. Acta* **1993**, *211*, 101.
(9) Sullivan, B. P.; Calvert, J. M.; Meyer, T. J. *Inorg. Chem.* **1980**, *19*, 1404.

S0020-1669(96)01061-0 CCC: $14.00

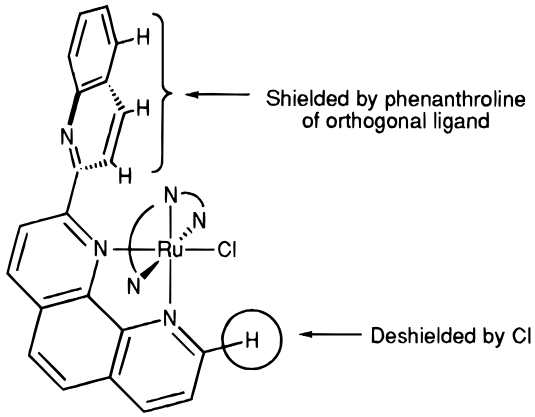

Figure 1. NMR Characteristics of structure **2**.

evidence formation of species **2**.[8] However, a more recent report from the same group describes the isolation of a didentate complex of 4-chloro-tpy having structure **2**.[10] These workers note that this species is thermally stable but photochemically isomerizes to structure **3**.

The isomerization of **2** to **3** may occur by a decoordination−recoordination process or by what is essentially a backside displacement of chloride by the unbound distal pyridine. In order to further probe the formation of these species as well as the isomerization process, we designed several analogous terdentate ligands in which the central and one distal pyridine are included in a 1,10-phenanthroline nucleus which should favor bidentate coordination. The remaining distal pyridine was replaced with a benzo-fused analogue, 2-quinolinyl or 1-isoquinolyl, providing ligands **4** and **5**. Both of these species allow

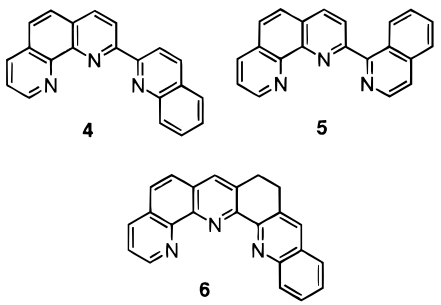

for rotation about the 2,2′-bond. A third ligand **6** was also prepared in which a 3,3′-dimethylene bridge restricts the appended 2-quinolinyl moiety to a *cisoid* geometry. This paper will report the coordination of **4**−**6** with Ru(II) and the involvement of species such as **2** and **3.**

Synthesis of the Ligands. Ligands **4**−**6** were prepared by employing the Friedländer condensation between 8-amino-7-quinolinecarbaldehyde (**7**) and an appropriate ketone. We have

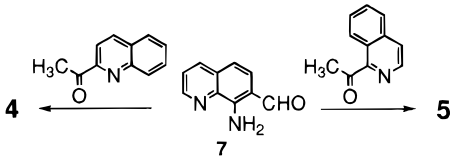

recently described an improved synthesis of **7**,[11] and the prerequisite ketones, 2-acetylquinoline[12] and 1-acetylisoquinoline,[13] were prepared according to published procedures. Terpyridine **4** could also be prepared by the reaction of 2-aminobenzaldehyde with 2-acetyl-1,10-phenanthroline, but the yield by this pathway was somewhat lower.

The precursor to **6**, 4-oxo-1,2,3,4-tetrahydroacridine (**10**), was prepared from 1,2,3,4-tetrahydroacridine by initial conversion to the 4-benzylidene derivative **9** followed by ozonolysis and

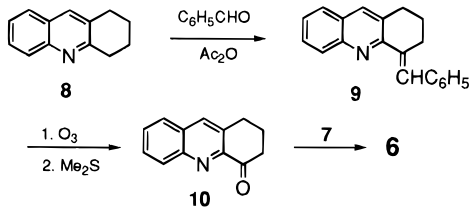

reduction of the ozonide with methyl sulfide. The ligands were all characterized by their ^{1}H and ^{13}C NMR spectra. The existence of numerous discrete, noninteracting spin systems facilitated a first-order analysis of these spectra.[14]

Complexation with Ru(II). Complexes of **4**−**6** were formed by the reaction of 2 equiv of the appropriate ligand with $RuCl_3 \cdot 3H_2O$ in either absolute ethanol or ethanol−water (1:1) at reflux for 8 h followed by precipitation of the complex as the hexafluorophosphate salt. In each case the crude reaction product was first analyzed by NMR where the presence of isomer **2** would be evidenced by the appearance of a peak at about 10.5 ppm, well downfield from other resonances. Further evidence for structure **2** was derived from the presence of peaks at approximately 6.0 and 6.5 ppm and attributed to protons on the uncoordinated quinoline or isoquinoline (see Figure 1). An approximate composition of **2**/**3** could be ascertained from the integrated area of these characteristic peaks versus others in the spectrum. The identity of both major and minor products was then established by chromatographic purification and a combination of analytical techniques.

For ligand **4**, the major product isolated in 70% yield was the pentaaza-coordinated (N5) species having structure **2**. In the crude reaction mixture less than 5% of the hexaaza-coordinated (N6) species with structure **3** could be identified. However, a 5 mg sample of this minor product could be isolated by column chromatography and it showed an ^{1}H NMR spectrum characteristic of $[Ru(\mathbf{4})_2]^{2+}$ where only one set of peaks for ligand **4** was observed. There was no evidence for conversion of structure **2** to **3** for this system.

For ligand **5**, the major product isolated in 63% yield was the N6 species $[Ru(\mathbf{5})_2]^{2+}$. The ^{1}H NMR of this complex was quite similar to the analogous minor product isolated from the reaction of ligand **4**. Chromatography on alumina allowed the isolation of the minor product (2 mg, 3%) which showed the characteristic shielded and deshielded protons for structure **2**. Once again, there was no evidence for the thermal conversion of the minor into the major product.

The dimethylene-bridged ligand **6** behaves differently from its unbridged analogue **4**. The N5 and N6 species were formed and isolated in approximately a 2:1 ratio. The N5 species was stable in the dark, but upon exposure to room light it slowly isomerized to the N6 complex.

As was observed for the parent terpyridine system, the N5 complex in every case appears pink while the N6 complex is purple in color. These differences are manifested in the electronic absorption spectra. Visible wavelength absorptions

(10) Constable, E. C.; Thompson, A. M. W. C. *Inorg. Chim. Acta* **1994**, *223*, 177.
(11) Riesgo, E. C.; Jin, X.; Thummel, R. P. *J. Org. Chem.* **1996**, *61*, 3017.
(12) Campbell, K. N.; Helbing, C. H.; Kerwin, J. F. *J. Am. Chem. Soc.* **1946**, *68*, 1840.
(13) Kaufmann, A.; Dandliker, P.; Burkhardt, H. *Ber.* **1913**, *46*, 2934.
(14) Ezell, E. L.; Thummel, R. P.; Martin, G. E. *J. Heterocycl. Chem.* **1984**, *21*, 817.

Table 1. Long-Wavelength Electronic Absorption Data for N5 and N6 Ru(II) Complexes

complex	λ_{max} (ϵ)[a]		
[Ru(**4**-*N*,*N*′,*N*′′)(**4**-*N*,*N*′)Cl]$^{1+}$	418 (7700)	493 (6370)	574 (5350)
[Ru(**4**-*N*,*N*′,*N*′′)$_2$]$^{2+}$	526 (4730)		
[Ru(**5**-*N*,*N*′,*N*′′)(**5**-*N*,*N*′)Cl]$^{1+}$	420 (7920)	493 (6610)	585 (4710)
[Ru(**5**-*N*,*N*′,*N*′′)$_2$]$^{2+}$	539 (9880)		
[Ru(**6**-*N*,*N*′,*N*′′)(**6**-*N*,*N*′)Cl]$^{1+}$	422 (2720)	504 (3320)	590 (2740)
[Ru(**6**-*N*,*N*′,*N*′′)$_2$]$^{2+}$	530 (6100)		

[a] Recorded in nm for 10^{-4} M solutions in CH_3CN at room temperature.

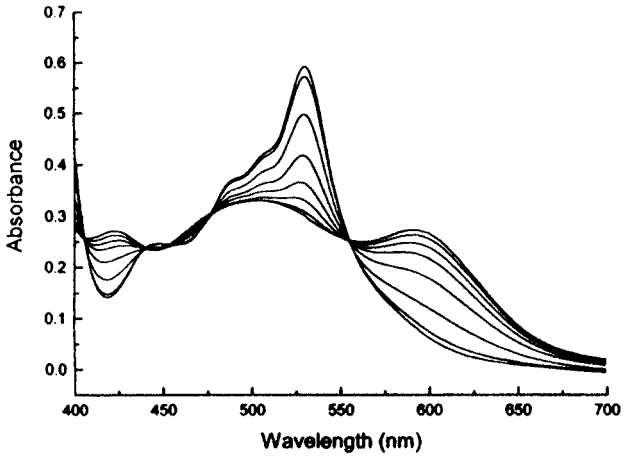

Figure 2. Electronic absorption spectra of [Ru(**6**-*N*,*N*′,*N*′′)(**6**-*N*,*N*′)-Cl](PF$_6$) in CH_3CN (9.71×10^{-5} M) at 25 °C recorded at $t = 0$, 1, 3, 6, 12, 25, 50, and 120 h.

for such complexes are generally associated with a metal-to-ligand charge transfer (MLCT) state, and the maxima of these peaks are recorded in Table 1. The N6 complexes all show a band similar to what is observed for [Ru(tpy)$_2$]$^{2+}$ but red-shifted due to the increased π-delocalization both in the phenanthroline and quinoline or isoquinoline moiety.[15] The N5 complexes show a set of three broad bands in the long wavelength region at about 420, 500, and 585 nm. Acetonitrile solutions of the complexes showed no detectable room-temperature luminescence when excited at their MLCT maxima.

The well-separated absorption maxima for the N5 and N6 complexes of ligand **6** allowed their interchange to be followed spectrophotometrically. Figure 2 illustrates a set of curves which were obtained starting with the N5 complex of **6** in acetonitrile over a period of 50 h at 25 °C. Five isosbestic points are observed, and the band at 591 nm for the N5 complex disappears as a new band for the N6 complex appears at 530 nm. Plotting the absorption data *versus* time for both peaks produced two parallel lines. Linear regression analysis provides a rate constant of 1.48×10^{-5} s^{-1} ($R = 0.997$) for loss of the peak at 591 nm while appearance of the peak at 530 nm provides a rate constant of 1.63×10^{-5} s^{-1} ($R = 0.998$). Both the clear appearance of isosbestic points as well as the close similarity of the rates point to a direct conversion from the N5 to N6 species or a process in which the intermediates are short lived.

The N5 species having structure **2** possess two chiral centers. Due to the asymmetry of the terdentate ligand, the metal center represents one chiral center. The second chiral center involves the disposition of the 2-substituent on the bidentate coordinated phenanthroline ring. Since this substituent is unsymmetrical about the axis of the 2,2′-bond, two rotamers, such as **4a**,**b**, may exist. The existence of both rotamers of the noncoordinated substituent leads to the appearance of two sets of NMR signals

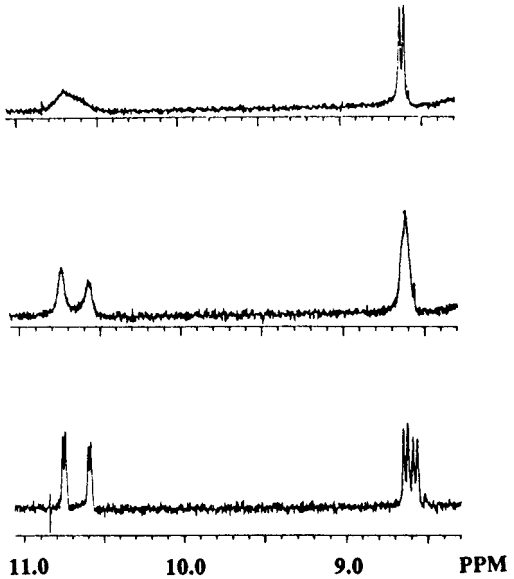

Figure 3. Downfield region of the 300 MHz ^{1}H NMR spectra of [Ru(**6**-*N*,*N*′,*N*′′)(**6**-*N*,*N*′)Cl](PF$_6$) in nitrobenzene-d_5, recorded at 22.4 °C (bottom), 60 °C (middle), and 80 °C (top).

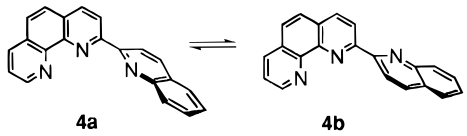

for each diastereomer. The dimethylene bridge in ligand **6** restricts the rotation around the 2,2′-bond to about ±20°; nevertheless two diastereoisomers are still observable. The lower energy barrier for the interconversion of these diastereomers allows this process to be observed by variable-temperature NMR. At 22.4 °C in nitrobenzene-d_5, the two lowest field signals in the ^{1}H NMR of the N5 complex of ligand **6** appear as a pair of approximately equal area doublets, one for each diastereomer (Figure 3). At 60 and 80 °C, these signals coalesce, allowing one to estimate an inversion barrier of about 17.5 kcal/mol for rotation about the 2,2′-bond in the complex.

To better understand the structure of the N5 species **2**, an X-ray crystal determination was carried out on [Ru(**4**-*N*,*N*′,*N*′′)-(**4**-*N*,*N*′)Cl](PF$_6$). An ORTEP plot of the cation is shown in Figure 4, and selected bond lengths, bond angles, and torsion angles are collected in Table 2. If one considers the coordinative bonds between ruthenium and the phen nitrogens, these are all approximately equal except for Ru−N4 which is shorter because it shares two chelate rings. The Ru−N16 bond is the longest since it involves the coordinated quinoline which is both more hindered and more flexible. Considering the chelation angles, the two N−Ru−N angles involving the phenanthrolines are almost identical but the N4−Ru−N16 angle involving quinoline is smaller in accord with the longer Ru−N16 bond.

The noncoordinated quinoline ring is twisted along the 2,2′-bond with a dihedral angle of 86.59° which compares to an angle of 3.23° for the coordinated quinoline. This orthogonality is also reflected in the 2,2′-bond length (C29−C39) which is 1.49 Å as compared with 1.45 Å for the corresponding bond on the coordinated quinoline. The most interesting feature is the π-stacked arrangement of the noncoordinated quinoline with respect to the phen portion of the terdentate ligand. The mean planes of the quinoline and phenanthroline are almost parallel, deviating by less than 5°. The average distance between these two planes is approximately 3.5 Å, which is optimal for effective $\pi-\pi$ interaction.

(15) Thummel, R. P.; Hegde, V.; Jahng, Y. *Inorg. Chem.* **1989**, *28*, 3264.

Table 2. Selected Bond Lengths, Bond Angles, and Torsional Angles for [Ru(**4**-*N*,*N*′,*N*″)(**4**-*N*,*N*′)Cl](PF_6)[a,b]

bond lengths (Å)		bond angles (deg)		dihedral angles (deg)	
Ru−Cl	2.395(2)	N25−Ru−N28	79.4(2)	C30−C29−C39−N40	86.59(0.85)
Ru−N1	2.086(6)	N1−Ru−N4	80.0(2)	N4−C5−C15−N16	3.23(0.83)
Ru−N4	1.962(6)	N4−Ru−N16	77.0(2)		
Ru−N16	2.141(6)	N4−Ru−N25	171.0(2)		
Ru−N25	2.076(6)	N28−Ru−Cl	170.1(2)		
Ru−N28	2.088(5)				
C29−C39	1.49(1)				
C5−C15	1.45(1)				

[a] Numbering pattern from Figure 4. [b] Numbers in parentheses are estimated standard deviations in the least significant digits.

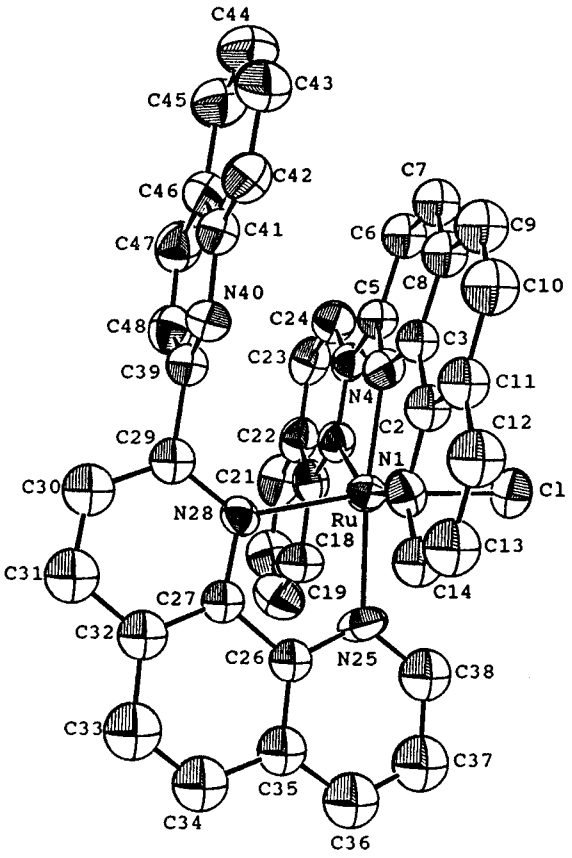

Figure 4. ORTEP drawing of the cation of [Ru(**4**-*N*,*N*′,*N*″)(**4**-*N*,*N*′)-Cl](PF_6) with atomic numbering scheme.

Discussion

The different coordination modes observed for **4** and **5** indicate that fairly subtle steric and electronic considerations can dictate the stereochemistry of binding. In both cases we assume the first coordination step involves formation of [Ru(*N*,*N*′,*N*″)Cl_3] (**1**) having no stereochemistry. In the second coordination step, as stated earlier, formation of the initial Ru−N bond involves a nitrogen on a distal ring, either the quinoline (or isoquinoline) nitrogen or N10 of the phenanthroline. The key feature therefore is axial *versus* equatorial attack on **1** or a solvated analogue of **1**. Equatorial attack will lead to bidentate coordination of the second ligand and formation of the N5 complex **2** while axial attack will lead to terdentate coordination of the second ligand and formation of the N6 complex **3**. We observe a strong bias for equatorial attack by **4** and axial attack by **5**. For ligand **4** initial attack at the equatorial position must involve N10 of phenanthroline. Examination of molecular models indicates that π-stacking between the appended quinoline and the already coordinated **4** could be important in stabilizing the activated complex leading to this mode of attack. However, similar π-stacking is also accessible to ligand **5** for the analogous mode of attack. In this latter case it is likely that the first coordination of the second ligand does not occur at the N10 of **5** but rather at the isoquinoline nitrogen which is now much less sterically encumbered than the quinoline nitrogen of **4** due to the more remote fusion of its benzo ring from the nucleophilic site. Equatorial attack by isoquinoline could not afford a N5 species because of the steric prohibition to binding N1 of the phenanthroline ring in an axial site.

The dimethylene ligand **6** provides a good test of this π-stacking theory since rotation about the 2,2′-bond of **6** is restricted to about $\pm 20°$, which would make π-stacking much less favorable. Indeed the amount of N5 complex **2** diminishes significantly from 20:1 to 2:1. It is interesting that thermal activation will allow flipping of the pendant quinoline ring while the complex remains intact as is evidenced by the variable-temperature NMR study (Figure 3). Photochemical activation, on the other hand, promotes decoordination which ultimately provides the thermodynamically favored N6 complex.

From a mechanistic standpoint the conversion of the N5 to N6 species can occur in two ways. The bidentate ligand in structure **2** could decoordinate and then recoordinate in a tridentate fashion with departure of chloride at some stage. This process could require as many as five separate decomplexation and recomplexation steps. A more appealing explanation, which is supported by the kinetic study, involves photodissociation of the chloride prior to, or concurrent with, backside attack by the uncoordinated quinoline ring. The fact that this process occurs more readily for **6** than **4** argues for a more concerted displacement process since, in the N5 complex of **6**, the quinoline is twisted so that its nitrogen lone pair electrons are oriented more toward the metal center, facilitating displacement. The relative ease of choride departure should be approximately equal for both systems.

An intriguing question arises as to whether formation of the N6 complex **3** always proceeds through initial formation of the N5 complex **2** followed by rearrangement. The thermal stability

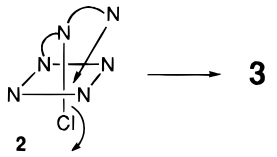

of some of these N5 complexes argues against such a common intermediate. Thus the major factor which dictates the formation of **2** versus **3** is axial or equatorial attack of the second ligand on intermediate **1**.

Further studies will address the importance of π-stacking effects in other similar coordination processes. The study of chiral Ru(II) complexes of unsymmetrical terdentate ligands is also being pursued.

Experimental Section

Melting points were measured on a Fisher-Johns melting points apparatus and are uncorrected. Nuclear magnatic resonance spectra (NMR) were obtained on a General Electric QE-300 spectrometer at

300 MHz for ^{1}H and 75 MHz for ^{13}C; chemical shifts are reported in parts per million downfield from Me_4Si referenced to the solvent peaks. UV−vis measurements were performed on a Perkin-Elmer Lambda 3B spectrophotometer. 2-Acetylquinoline,[12] 2-acetylisoquinoline,[13] 2-acetyl-1,10-phenanthroline,[16] 1,2,3,4-tetrahydroacridine,[17] and 8-amino-7-quinolinecarbaldehyde[11] were synthesized according to a known procedure or a modification of such a method. Chemicals and solvents were commercial reagent grade and used without further purification.

4-Benzylidene-1,2,3,4-tetrahydroacridine (9). A mixture of 1,2,3,4-tetrahydroacridine (10.3 g, 0.056 mol), freshly distilled benzaldehyde (10.0 g, 0.092 mol), and Ac_2O (20 mL) was refluxed for 24 h. The solvent was removed by distillation, and the oily residue was dissolved in CH_2Cl_2 (80 mL) and washed with 50% KOH, followed by H_2O. The organic layer was dried over anhydrous $MgSO_4$. Evaporation of the solvent gave a solid which was washed with cold hexane (5 × 10 mL) to give 14.83 g (95%) of a white solid, mp 103−104 °C: ^{1}H NMR ($CDCl_3$) δ 8.22 (s, 1H), 8.08 (d, 1H, J = 8.4 Hz, H_5), 7.84 (s, 1H), 7.71 (d, 1H, J = 7.8 Hz, H_8), 7.63 (t, 1H, J = 7.2 Hz, H_7), 7.52−7.47 (m, 2H), 7.44−7.38 (m, 3H), 7.28 (td, 1H, J = 7.5, 0.9 Hz, H_6), 3.03 (t, 2H, J = 5.1 Hz), 3.01 (t, 2H, J = 5.1 Hz), 1.92 (quintet, 2H, J = 5.7 Hz).

4-Oxo-1,2,3,4-tetrahydroacridine (10). A solution of 4-benzylidene-1,2,3,4-tetrahydroacridine (7.37 g, 0.027 mol) in CH_2Cl_2 (300 mL) was cooled in a dry ice−acetone bath, and an O_3/O_2 mixture was bubbled into the solution until a blue color persisted. After the purging of excess O_3/O_2, $(CH_3)_2S$ (6 mL) was added and the resulting mixture was allowed to warm to room temperature and stirred overnight. The CH_2Cl_2 and excess $(CH_3)_2S$ were evaporated, and the residue was redissolved in CH_2Cl_2 (200 mL) and washed with water, followed by brine. The organic layer was dried over $MgSO_4$. Evaporation of the solvent gave 6.12 g of sticky material, which was chromatographed on silica gel (15 g) eluting with hexane/CH_2Cl_2 (4:1). The latter fractions gave 3.30 g (60%) of **10** as white crystals, mp 144−145 °C: ^{1}H NMR ($CDCl_3$) δ 8.32 (d, 1H, J = 8.4 Hz, H_5), 8.90 (s, 1H, H_9), 7.78 (d, 1H, J = 8.1 Hz, H_8), 7.71 (t, 1H, J = 7.5 Hz, H_6 or H_7), 7.59 (t, 1H, J = 7.5 Hz, H_6 or H_7), 3.19 (t, 2H, J = 6.0 Hz), 2.91 (t, 2H, J = 6.6 Hz), 2.24 (quintet, 2H, J = 6.3 Hz); ^{13}C NMR ($CDCl_3$) δ 197.22, 148.35, 141.19, 136.24, 135.88, 131.05, 129.62, 129.31, 128.71, 126.76, 40.37, 29.35, 22.61. Anal. Calcd for $C_{13}H_{11}NO$: C, 79.19; H, 5.58; N, 7.11. Found: C, 79.03; H, 5.57; N, 7.13.

2-(2′-Quinolyl)-1,10-phenanthroline (4). Method A. A mixture of 2-acetylquinoline (0.52 g, 0.003 mol), 8-aminoquinoline-7-carbaldehyde (0.52 mg, 0.003 mol), and saturated ethanolic KOH (1.0 mL) in absolute EtOH (15 mL) was refluxed for 8 h. The solvent was evaporated, and the residue was dissolved in CH_2Cl_2 (80 mL). The solution was washed with water (3 × 20 mL) and dried over anhydrous $MgSO_4$. Evaporation of the solvent gave 0.96 g of a yellow solid, which was chromatographed on alumina eluting with hexane/CH_2Cl_2 (1:4). The early fractions afforded 0.83 g (90%) of **4**, mp 194−195 °C (lit.[16] mp 194 °C): ^{1}H NMR ($CDCl_3$) δ 9.28 (dd, 1H, J = 4.2, 1.2 Hz), 9.17 (d, 1H, J = 8.7 Hz), 9.09 (d, 1H, J = 8.4 Hz), 8.43 (d, 1H, J = 8.4 Hz), 8.38 (d, 1H, J = 8.7 Hz), 8.29 (d, 1H, J = 8.1 Hz), 8.24 (d, 1H, J = 8.7 Hz), 7.90 (d, 1H, J = 8.4 Hz), 7.88 −7.80 (AB quartet, 2H), 7.56 (t, 1H, J = 8.4 Hz), 7.67 (dd, 1H, J = 8.1, 4.5 Hz), 7.58 (t, 1H, J = 7.5 Hz).

Method B. A mixture of 2-acetyl-1,10-phenanthroline (119 mg, 0.5 mmol), 2-aminobenzaldehyde (61 mg, 0.5 mmol), and saturated ethanolic KOH (1.0 mL) in absolute EtOH (15 mL) was refluxed for 8 h. Workup as described in method A afforded 0.075 g (50%) of 2-(2′-quinolyl)-1,10-phenanthroline, mp 188−189 °C: spectral data were identical to those reported for method A.

2-(1′-Isoquinolyl)-1,10-phenanthroline (5). A mixture of 1-acetylisoquinoline (51.6 mg, 3 mmol), 8-aminoquinoline-7-carbaldehyde (51.3 mg, 3 mmol), and saturated ethanolic KOH (3.0 mL) in absolute EtOH (20 mL) was refluxed for 8 h. The solvent was evaporated, and the residue was dissolved in CH_2Cl_2 (80 mL). The solution was washed with water (3 × 20 mL) and dried over anhydrous $MgSO_4$. Evaporation of the solvent gave 1.00 g of a yellow solid, which was chromatographed on alumina (25g) eluting with hexane/CH_2Cl_2 (3:7). The early fractions gave 0.65 g (75%) of **5** as white needles, mp 185−186 °C: ^{1}H NMR ($CDCl_3$) δ 9.13 (dd, 1H, J = 4.2, 1.2 Hz, H_9), 8.98 (d, 1H, J = 8.4 Hz, H_3), 8.62 (d, 1H, J = 5.7 Hz, H_3), 8.35−8.28 (AB quartet, 2H, H_5, H_6), 8.15 (dd, 1H, J = 8.1, 1.2 Hz, H_7), 7.81 (d, 1H, J = 7.8 Hz), 7.77−7.70 (AB quartet, 2H), 7.67−7.52 (overlapping m, 4H); ^{13}C NMR ($CDCl_3$) δ 157.9, 157.4, 150.2, 146.2, 145.0, 141.6, 137.0, 136.6, 135.8, 129.9, 128.7, 128.2, 127.9, 127.8, 127.4, 126.9, 126.6, 126.1, 124.5, 122.8, 121.4. Anal. Calcd for $C_{21}H_{13}N_3$: C, 82.09; H, 4.23; N, 13.68. Found: C, 81.97; H, 4.36; N, 13.49.

3,3′-Dimethylene-2-(2′-quinolyl)-1,10-phenanthroline (6). A mixture of 4-oxo-1,2,3,4-tetrahydroacridine (**10**, 0.20 g, 1.0 mmol), 8-amino-7-quinolinecarbaldehyde (0.17 g, 1.0 mmol), and saturated ethanolic KOH (1.0 mL) in absolute EtOH (15 mL) was refluxed for 8 h. The solvent was evaporated, and the residue was dissolved in CH_2Cl_2 (80 mL). The solution was washed with water (3 × 20 mL) and dried over anhydrous $MgSO_4$. Evaporation of the solvent gave 1.00 g of a yellow solid which was recrystallized from hexane/$CHCl_3$ (2:1) to afford 0.28 g (84%) of **6**, mp 264−265 °C: ^{1}H NMR ($CDCl_3$) δ 9.23 (dd, 1H, J = 4.5, 1.5 Hz, H_9), 8.53 (d, 1H, J = 8.4 Hz, $H_{8'}$), 8.25 (dd, 1H, J = 8.1, 1.5 Hz), 8.07 (s, 1H, H_4 or $H_{4'}$), 8.00 (s, 1H, $H_{4'}$ or H_4), 7.78−7.71 (m, 4H), 7.65 (dd, J = 8.1, 4.5 Hz, H_8), 7.54 (t, 1H, J = 7.5 Hz), 3.26 (broad s, 4H); ^{13}H CNMR ($CDCl_3$) δ 152.0, 151.5, 149.8 (2 C's), 147.8, 146.5, 145.3, 136.6, 135.0, 134.9, 132.3, 130.0, 129.6, 129.0, 128.8, 128.5, 127.4, 127.3, 126.9, 126.3, 123.2, 28.3 (2 C's). Anal. Calcd for $C_{23}H_{15}N_3 \cdot 0.75H_2O$: C, 79.65; H, 4.76; N, 12.12. Found: C, 79.58; H, 4.86; N, 12.39.

[Ru(4-*N*,*N*′,*N*″)(4-*N*,*N*′)Cl](PF$_6$) and [Ru(4-*N*,*N*′,*N*″)$_2$](PF$_6$)$_2$. A mixture of 2-(2′-quinolyl)-1,10-phenanthroline (**4**, 158.5 mg, 0.51 mmol) and $RuCl_3 \cdot 3H_2O$ (65 mg, 0.25 mmol) in absolute EtOH (25 mL) was refluxed for 8 h. After being cooled to room temperature, the reaction mixture was filtered to give 68.6 mg of dark brown solid. To the filtrate was added NH_4PF_6 (90 mg, 55 mmol), and the precipitate formed was collected to give 162 mg of brownish-red solid, which was chromatographed on alumina (20 g) eluting with CH_3CN/toluene (1:1). The early fractions (red-purple band, R_f = 0.55) gave 157 mg (70%) of [Ru(**4**-*N*,*N*′,*N*″)(**4**-*N*,*N*′)Cl](PF$_6$) as a 3.5:6.5 mixture of two diastereomers: ^{1}H NMR (CD_3CN) δ 10.68 (d, J = 5.1 Hz, 1H), 10.64 (d, J = 5.4 Hz, 1H), 9.06 (d, J = 8.1 Hz, 2H), 8.57−8.46 (three overlapping d, 4H), 8.40−8.23 (m, 8H), 8.14−8.07 (AB quartet, 2H), 8.04−7.91 (m, 6H), 7.89−7.63 (m, 8H), 7.53−7.44 (m, 4H), 7.38−7.24 (m, 6H), 7.19−7.07 (overlapping m, 5H), 7.00 (d of dd, 1H, J = 8.7, 7.2, 0.9 Hz), 6.95 (d, 1H, J = 5.4 Hz), 6.79 (d, 1H, J = 8.1 Hz), 5.91 (d, 1H, J = 8.4 Hz), 5.85 (d, 1H, J = 8.1 Hz). Anal. Calcd for $C_{42}H_{26}N_6ClF_6PRu \cdot 2H_2O$: C, 54.11; H, 3.22; N, 9.02. Found: C, 54.17; H, 3.55; N, 8.93. The latter fractions (pink-red band, R_f < 0.1) gave 5 mg (2%) of [Ru(**4**-*N*,*N*′,*N*″)$_2$](PF$_6$)$_2$ as red crystals: ^{1}H NMR (CD_3CN) δ 9.50 (d 1H, J = 8.4 Hz,), 9.15 (d, 1H, J = 8.7 Hz), 8.94 (d, 1H, J = 9.0 Hz), 8.57 (d, 1H, J = 8.4 Hz), 8.51 (d, 1H, J = 9.0 Hz), 8.28 (d, 1H, J = 7.5 Hz), 8.21 (d, 1H, J = 9.0 Hz), 7.80 (d, 1H, J = 8.4 Hz), 7.40 (t, 1H, J = 7.8 Hz), 7.24 (dd, 1H, J = 8.1, 5.1 Hz), 7.15 (t, 1H, J = 8.4 Hz), 7.04 (d, 1H, J = 5.7 Hz), 6.94 (d, 1H, J = 8.4 Hz, $H_{8'}$).

[Ru(5-*N*,*N*′,*N*″)(5-*N*,*N*′)Cl](PF$_6$) and [Ru(5-*N*,*N*′,*N*″)$_2$](PF$_6$)$_2$. A mixture of 2-(1′-isoquinolyl)-1,10-phenanthroline (**5**, 49.4 mg, 0.16 mmol) and $RuCl_3 \cdot 3H_2O$ (20.9 mg, 0.08 mmol) in absolute EtOH (10 mL) was refluxed for 8 h. The reaction mixture was cooled to room temperature and filtered. Evaporation of the purple-red filtrate afforded 51.2 mg of purple red solid, which was chromatographed on alumina (20 g) eluting with EtOH/CH_3CN (1:19). The early fractions (R_f = 0.45) afforded 2 mg (3%) of [Ru(**5**-*N*,*N*′,*N*″)(**5**-*N*,*N*′)Cl]Cl. The latter fractions (R_f = 0.3) gave [Ru(**5**-*N*,*N*′,*N*″)$_2$]Cl$_2$, which was precipitated with excess NH_4PF_6 (40 mg) in EtOH (5 mL) to give 45 mg (63%) of purple-red precipitate as a [Ru(**5**-*N*,*N*′,*N*″)$_2$](PF$_6$)$_2$: ^{1}H NMR (CD_3CN) δ 9.68 (d, 1H, J = 9.0 Hz, H_3), 9.34 (d, 1H, J = 9.0 Hz, $H_{8'}$), 9.04 (d, 1H, J = 9.8 Hz, H_4), 8.53 (d, 1H, J = 9.0 Hz, H_5 or H_6), 8.41 (d, 1H, J = 8.4 Hz, H_7), 8.29 (d, 1H, J = 9.0 Hz, H_6 or H_5), 8.04 (ddd, 1H, J = 9.0, 6.6, 1.2 Hz, $H_{7'}$), 7.92 (t, 1H, J = 7.5 Hz, $H_{5'}$ or $H_{6'}$), 7.87 (t, 1H, J = 8.1 Hz, $H_{5'}$ or $H_{6'}$), 7.47 (d, 1H, J = 5.1 Hz, H_9), 7.44 (d, 1H, J = 6.3 Hz, $H_{3'}$), 7.30 (dd, 1H, J = 8.4, 5.1 Hz, H_8), 7.24 (d, 1H, J = 6.0 Hz, $H_{4'}$). Anal. Calcd for $C_{42}H_{26}N_6RuF_{12}P_2$: C, 50.15; H, 2.59;

(16) Case, F. H.; Schilt, A. A. *J. Heterocycl. Chem.* **1979**, *16*, 1135.
(17) (a) Borsche, W.; Tiedtke, H.; Schmidt, R *Justus Liebigs Ann. Chem.* **1910**, *377*, 78. (b) Tilak, B. D.; Berde, H.; Gogte, V. N.; Ravindranathan, T. *Indian J. Chem*. **1970**, *8*, 1.

N, 8.36. Found: C, 50.16; H, 2.68; N, 8.30. The pentacoordinate complex, [Ru(**5**-*N*,*N*′,*N*′′)(**5**-*N*,*N*′)Cl]Cl, was also converted to PF_6 salt and one of the two diastereomers was isolated: ^{1}H NMR (CD_3CN) δ 10.48 (dd, 1H, J = 4.8, 1.2 Hz), 9.20 (d, 1H, J = 8.1 Hz), 8.96 (dd, 1H, J = 8.1, 1.2 Hz), 8.81 (d, 1H, J = 9.0 Hz), 8.51 (d, 1H, J = 8.7 Hz), 8.45 (d, 1H, J = 8.1 Hz), 8.34−8.29 (m, 2H), 8.15 (d, 1H, J = 8.4 Hz), 8.08−8.01 (m, 2H), 7.90 (d, 1H, J = 7.5 Hz), 7.87−7.83 (m, 2H), 7.79−7.72 (m, 3H), 7.58−7.50 (m, 3H), 7.45 (d, 1H, J = 4.8 Hz), 7.40 (d, 1H, J = 7.8 Hz), 7.23 (t, 1H, J = 8.4 Hz), 7.18 (d, 1H, J = 8.1 Hz), 6.43 (dd, 1H, J = 7.8, 6.6 Hz), 5.93 (d, 1H, J = 8.1 Hz).

[Ru(6-*N*,*N*′,*N*′′)(6-*N*,*N*′)Cl](PF$_6$) and [Ru(6-*N*,*N*′,*N*′′)$_2$](PF$_6$)$_2$. A mixture of 3,3′-dimethylene-2-(2′quinolyl)-1,10-phenanthroline (**6**, 111.0 mg, 0.33 mmol) and $RuCl_3 \cdot 3H_2O$ (43.6 mg, 0.166 mmol) in absolute EtOH (15 mL) was refluxed for 8 h. After cooling of the reaction mixture in the refrigerator, the reaction mixture was filtered. The filtrate was precipitated with excess NH_4PF_6 in EtOH. The dark red precipitate was filtered and chromatographed on alumina eluting with CH_3CN/toluene (1:1). The early purple fraction (R_f = 0.5) gave 57 mg (35%) of [Ru(**6**-*N*,*N*′,*N*′′)(**6**-*N*,*N*′)Cl](PF$_6$) as a 5.5:4.5 mixture of two diastereomers: ^{1}HNMR (CD_3CN) δ 10.64 (d, 1H, J = 5.1 Hz), 10.43 (d, 1H, J = 5.1 Hz), 8.51 (d, 1H, J = 8.1 Hz), 8.46 - 8.43 (m, 2H), 8.39 (dd, 1H, J = 7.2, 1.8 Hz), 8.38 (d, 1H, J = 9.0 Hz), 8.32 (d, 1H, J = 5.1 Hz), 8.29 (s, 2H), 8.14−8.05 (m, 5H), 8.08−7.92 (m, 4H), 7.87 (s, 1H), 7.84 (d, 1H, J = 7.8 Hz), 7.76 (d, 1H, J = 8.1 Hz), 7.72−7.64 (m, 5H), 7.58 (t, 1H, J = 7.5 Hz), 7.53−7.45 (m, 2H), 7.31 (d, 1H, J = 7.2 Hz), 7.28−7.14 (m, 7H), 7.02 (dd, 1H, J = 8.1, 5.1 Hz), 6.68 (td, 1H, J = 7.8, 0.9 Hz), 6.31 (d, 1H, J = 5.1 Hz), 6.26 (d, 1H, J = 8.7 Hz), 6.01 (d, 1H, J = 5.7 Hz), 5.81 (d, 1H, J = 8.4 Hz), 3.33−3.00 (m, 8H). The latter red fractions (R_f = 0.35) afforded 32 mg (18%) of [Ru(**6**-*N*,*N*′,*N*′′)$_2$](PF$_6$)$_2$: ^{1}H NMR (CD_3CN) δ 8.84 (s, 1H), 8.45 (d, 1H, J = 9.0 Hz), 8.27 (s, 1H), 8.25 (d, 1H, J = 8.1 Hz), 8.17 (d, 1H, J = 9.0 Hz), 7.72 (d, 1H, J = 8.1 Hz), 7.36 (t, 1H, J = 7.5 Hz), 7.23 (dd, 1H, J = 8.1, 4.8 Hz, H_8), 7.16 (d, 1H, J = 8.1 Hz), 7.10 (d, 1H, J = 4.8 Hz), 6.72 (d, 1H, J = 8.7 Hz), 3.96 (m, 2H), 3.76 (m, 2H). Anal. Calcd for $C_{46}H_{30}N_6RuF_{12}P_2$: C, 52.22; H, 2.84; N, 7.95. Found: C, 52.11; H, 2.97; N, 7.95.

Kinetic Measurements. A stock solution (0.97×10^{-5} M) of Ru[(**6**-*N*,*N*′,*N*′′)(**6**-*N*,*N*′)Cl](PF$_6$) in CH_3CN was prepared and placed in a flask under room light. The stock solution can be stored in the dark without any change for 1 month.

The spectrophotometer was equilibrated and calibrated from 700 to 400 nm against a visible source. Every 60 min, a 3 mL aliquot was removed from the solution, placed in a 1 × 1 × 3 cm cuvette, and immediately scanned over the range from 700 to 400 nm. The aliquot was was then returned to the solution flask. Rate data for the conversion were obtained by monitoring the absorbance increase at 530 nm and absorbance decrease at 591 nm. A first-order rate constant, k, was calculated according to a linear least-squares regression analysis:

$$\ln |A_f - A_t| = -kt + \ln |A_f - A_0|$$

Here A_f is the final absorbance of the sample solution, which is same as the absorbance of the N6 complex, and A_0 is the initial absorbance of the stock solution. A_t is the absorbance measured at time t.

X-ray Determination. Data were collected on an Enraf-Nonius CAD-4 diffractometer using the ω scan technique, Mo Kα radiation (λ = 0.717 03 Å), and a graphite monochromator. Standard procedures for data collection have been described previously.[18] Pertinent details are given in Table 3. Data were corrected for Lorentz and polarization effects and absorption using a ψ-scan (correction factors 0.92/0.99). The structure was solved using Patterson and Fourier techniques and the model refined using full-matrix least-squares techniques. All non-hydrogen atoms except the carbons of the fused three-ring systems were treated with anisotropic thermal parameters. Hydrogen atoms were located on difference maps, and then included in the model in idealized positions (U(H) = $1.3B_{eq}$(C)). All computations were performed using MolEN.[19] Scattering factors were taken from the usual sources.[20]

Table 3. Data Collection and Processing Parameters for the X-ray Structure Determination of [Ru(**4**-*N*,*N*′,*N*′′)(**4**-*N*,*N*′)Cl](PF$_6$)

molecular formula	$C_{42}H_{26}C1F_6N_6PRu$
size (mm)	0.09 × 0.21 × 0.24
temp (K)	293
space group	$C2/c$
a (Å)	29.308(3)
b (Å)	15.205(2)
c (Å)	19.505(2)
α (deg)	90
β (deg)	107.312(8)
γ (deg)	90
V (Å^3)	8298(1)
Z	8
D_c (g/cm^3)	1.435
μ (cm^{-1})	5.35
$2\theta_{max}$ (deg)	44
tot. reflcns	5417
unique reflcns	5310
R_{int}	0.031
reflcns with $I \geq 3\sigma(I)$	3281
params	438
R, R_w[a]	0.0502, 0.0659
$(\Delta/\sigma)_{max}$	<0.02
ρ_{min}, ρ_{max}	0.50, −0.41

[a] $R = \sum(|F_o| - |F_c|)/\sum(|F_o|)$; $R_w = [w\sum(|F_o| - |F_c|)^2/w\sum(|F_o|)^2]^{1/2}$, where $w = [0.04F^2 + (\sigma F)^2]^{-1}$.

Acknowledgment. For financial support of this work, R.P.T. (Grant E- 621) and S.B. (Grant B-1202) thank the Robert A. Welch Foundation. R.P.T. also thanks the National Science Foundation (Grant CHE-9224686) and the Texas Higher Education Coordinating Board. S.G.B. thanks the UNT Research Office, and Y.J. thanks the Korean Research Foundation. We are also grateful to Feiyue Wu and John Hazelrigg for assistance.

Supporting Information Available: Tables of crystallographic data and anisotropic parameters for [Ru(**4**-*N*,*N*′,*N*′′)(**4**-*N*,*N*′)Cl](PF$_6$) and a plot of ln $|A_\infty - A_t|$ versus time for 530 and 591 nm absorbances of [Ru(**6**-*N*,*N*′,*N*′′)(**6**-*N*,*N*′)Cl](PF$_6$) (10 pages). Ordering information is given on any current masthead page.

IC961061U

(18) Mason, M. R.; Smith, J. M.; Bott, S. G.; Barron, A. R. *J. Am Chem. Soc.* **1993**, *115*, 4971.
(19) *MolEN, An Interactive Structure Solution Program*; Enraf-Nonius: Delft, The Netherlands, 1990.
(20) Cromer, D. T.; Waber, J. T. *International Tables for X-ray Crystallography;* Kynoch Press: Birmingham, U.K., 1974; Vol. IV, Table 2.